# Fluidic trapping of deformable polymers in microflows

Nobuhiko Watari*
*Macromolecular Science and Engineering Center, University of Michigan, Ann Arbor, Michigan 48109-2136, USA*

Masao Doi
*Department of Applied Physics, The University of Tokyo, Bunkyo-ku, Tokyo 113-8656, Japan*

Ronald G. Larson
*Department of Chemical Engineering, Macromolecular Science and Engineering Center, University of Michigan, Ann Arbor, Michigan 48109-2136, USA*

(Received 20 October 2007; revised manuscript received 12 May 2008; published 10 July 2008)

We report that a polymer molecule can be trapped spatially and conformationally using a microflow that has at least two stagnation points (or two points with equal velocity) and a net flow orthogonal to the line connecting them. Examples include a Taylor vortex flow and an electro-osmotic flow in a channel with surfaces that have a sinusoidal charge. Simulating the motion of a polymer molecule in these flows using Brownian dynamics, we find that such flows produce a curved polymer conformation, leading to an elastic force that drives migration against the flow, thus stabilizing this conformation. Simulations with hydrodynamic interactions confirm these predictions and show that there exists a repulsive interaction between two trapped polymers.

DOI: 10.1103/PhysRevE.78.011801 PACS number(s): 36.20.−r, 83.10.Mj

## I. INTRODUCTION

The dynamics of a polymer molecule in a microflow can be drastically different from that in a uniform flow field. Here, we refer to a microflow as a flow field with a significant variation of velocity gradient over length scales of microns, which are typical dimensions of long bio-polymers such as DNA. In such a flow, the conformation of a polymer molecule can be strongly affected by the the structure of the velocity gradient field, which is not uniform over the length scale of the molecule as is the case of macroscopic flows. This is because each segment of the molecule can be subjected to a different velocity gradient due to the rapid variation in velocity.

When a long polymer molecule is placed in an extensional flow, a hysteretic conformational transition (the "coil-stretch transition") can occur as a function of flow strength [1]. This transition can also occur in a microflow, as was demonstrated by simulations of a polymer tethered to a wall at the stagnation point of an extensional flow field above the wall [2]. As another example, it was predicted by simulations that a coil-stretch transition can be controlled by a combination of counter rotating vortexes and an attractive potential from a plane wall [3].

We report here that a polymer molecule can be trapped both spatially and conformationally using only a microflow which has at least two stagnation points (or two points with equal velocity) and a net flow orthogonal to the line connecting them. Such microflows are likely to be common in microfluidic devices in which the velocity gradient can vary significantly over the length scale of the polymer. One example considered in this paper is a Taylor vortex velocity field (Fig. 1) [4]. The spatial and conformational trapping in a microflow indicates that a microflow can generate a nonuniform probability distribution of polymer in the position-conformation phase space. When this nonuniformity varies with the size of molecule, this can be used for molecule separations.

Below, the simulation methods and the model for a polymer molecule are presented (Sec. II B), followed by the results in Taylor vortex flow (Sec. III A) and an electro-osmotic flow in a microchannel (Sec. III C). Also, the effect of hydrodynamic interaction (HI) is discussed for trapping of a single molecule and for simultaneous trapping of two molecules in Sec. III B.

## II. METHOD

### A. Taylor vortex flow

Taylor vortex flow (Fig. 1) is an incompressible flow field and can be expressed in terms of a scalar stream function $\Psi(x,y)$ as [4]:

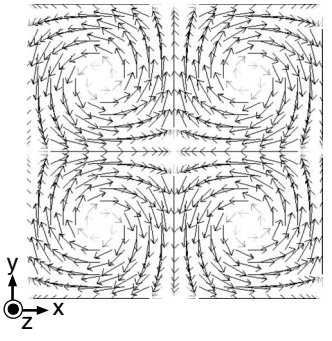


FIG. 1. Taylor vortex flow field. Drawn for the region $(x,y)=([0,\alpha],[0,\alpha])$. The velocity component of the $z$ direction is always zero.

*nobuhiko@umich.edu

 

$$\Psi(x,y) = \frac{A\alpha\beta}{2\pi}\cos(2\pi x/\alpha)\cos(2\pi y/\beta), \tag{1}$$

$$v_x(x,y) = \frac{\partial\Psi}{\partial y} = -A\alpha\cos(2\pi x/\alpha)\sin(2\pi y/\beta), \tag{2}$$

$$v_y(x,y) = -\frac{\partial\Psi}{\partial x} = A\beta\sin(2\pi x/\alpha)\cos(2\pi y/\beta), \tag{3}$$

$$v_z(x,y) = 0. \tag{4}$$

Although without a driving force the Taylor vortex decays with time due to viscosity, this decay is ignored here and $\beta$ is assumed to be equal to $\alpha$, for simplicity. Therefore, the only parameters required to specify the flow field are the magnitude of the flow velocity $A$ and the wavelength $\alpha$.

### B. Brownian dynamics

Using Taylor vortex velocity field, we compute the three-dimensional motion and deformation of a polymer molecule with the Brownian dynamics (BD) simulation. A bead-spring model is employed to represent the polymer molecule and the following equation of motion is computed for each bead [5]:

$$\boldsymbol{r}_i(t+\delta t) - \boldsymbol{r}_i(t) = \boldsymbol{v}_i(\boldsymbol{r}_i)\,\delta t + \frac{\boldsymbol{f}_i}{\xi}\delta t + \sqrt{6\frac{\delta t k_B T}{\xi}}\boldsymbol{n}. \tag{5}$$

Here, $\boldsymbol{r}_i$, $\boldsymbol{v}_i$, and $\boldsymbol{f}_i$ are the position, velocity, and conservative force vectors of bead $i(=0\rightarrow N)$, respectively, where $\boldsymbol{v}_i(\boldsymbol{r}_i)$ is given by Eqs. (2)–(4). $\delta t$ is the time increment of the simulation, $\xi$ is the drag coefficient of each bead, $k_B$ is the Boltzmann constant, $T$ is the absolute temperature, and $\boldsymbol{n}$ is a random vector whose components are chosen from the range $[-1,1]$ in each time step. This is a free-draining BD simulation with hydrodynamic interactions (HIs) between beads ignored. The effect of HI is discussed in Sec. III B.

We take the force of the spring, which connects the adjacent beads $i$ and $j$, to be that of a WLC (worm-like-chain) [6–8] used to model semiflexible polymers such as a DNA:

$$\boldsymbol{f}_{ij}^{\mathrm{sp}} = \frac{k_B T}{2b_K}\left\{\left(1-\frac{r_{ij}}{R_0}\right)^{-2} - 1 + \frac{4r_{ij}}{R_0}\right\}\frac{\boldsymbol{r}_{ij}}{r_{ij}}, \tag{6}$$

where $\boldsymbol{r}_{ij}=\boldsymbol{r}_i-\boldsymbol{r}_j$, $b_K$ is the Kuhn length of the polymer, and $R_0=L/(N-1)$ is the maximum spring length where $L$ is the contour length of the molecule. The force due to the excluded volume of beads is modeled as [8]:

$$\boldsymbol{f}_{ij}^{\mathrm{ex}} = -\frac{\partial U_{ij}^{\mathrm{ex}}}{\partial \boldsymbol{r}_{ij}} \tag{7}$$

with

$$U_{ij}^{\mathrm{ex}} = \frac{1}{2}\upsilon k_B T N_{K,s}^2\left(\frac{3}{4\pi S_s^2}\right)^{3/2}\exp\left(-\frac{3r_{ij}^2}{4S_s^2}\right), \tag{8}$$

where $\upsilon$ is the excluded volume parameter, and $S_s^2 = N_{K,s}b_K^2/6$ is the radius of gyration of an ideal chain consisting of $N_{K,s}$ Kuhn segments, with $N_{K,s}$ related to the spring length $R_0$ by $R_0=N_{K,s}b_K$. The total conservative force acting on bead $i$ is $\boldsymbol{f}_i=\Sigma_j(\boldsymbol{f}_{ij}^{sp}+\boldsymbol{f}_{ij}^{ex})$.

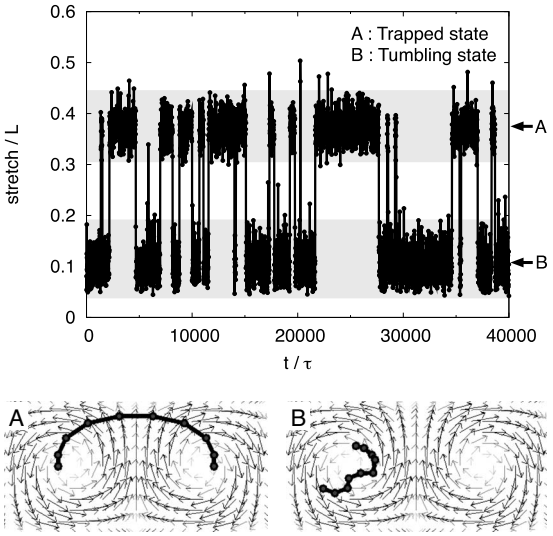


FIG. 2. A stretch history of a polymer molecule in a Taylor vortex flow with $A\alpha=2.0[l/\tau]$, $\alpha=12[l]$ (top). The polymer takes two states: the trapped state (left bottom) and the tumbling state (right bottom). The polymer molecule has contour length $L=21[l]$ (10 beads) and the stretch is defined as the largest distance between any two beads in a molecule.

In what follows, we take $l$, $k_BT$, and $\tau$ as the units of length, energy, and time, respectively, and here we set $l=1(\mu\mathrm{m})$, and $\tau=1(\mathrm{s})$. In our simulations, the time increment of the polymer motion is $\delta t=0.01[\tau]$. The drag coefficient of a bead is $\xi=11.9[k_\mathrm{B}\mathrm{T}\tau/l^2]$. The contour length of the polymer molecule is $L=21.0[l]$ and the polymer contains 10 beads. The Kuhn length is $b_K=0.106[l]$ and excluded volume parameter $\upsilon=0.0012[l^3]$. These parameters for the WLC spring model and the excluded volume potential were taken from Ref. [8] to model a λ-DNA molecule.

## III. RESULTS

### A. Trapping in a Taylor vortex flow

The BD simulations for a polymer in a Taylor vortex flow show that the molecule can exist in two types of state, the conformationally trapped and the tumbling state (see Fig. 2). In the tumbling state, the polymer molecule rotates in a vortical region of the flow. In the trapped state, the polymer molecule is held roughly stationary both spatially and conformationally long enough to be tracked for many polymer relaxation times even in the presence of Brownian motions.

This phenomenon is analogous to the coexistence of both coiled and stretched states of a polymer tethered to a plane wall and subjected to a stagnation point flow [2]. In this microflow, the tethered polymer can exist in either a coiled or stretched state, since in the stretched state, the free end of the polymer resides in a fast flow that keeps the chain stretched, while in the coiled state, the whole molecule resides near the stagnation point.

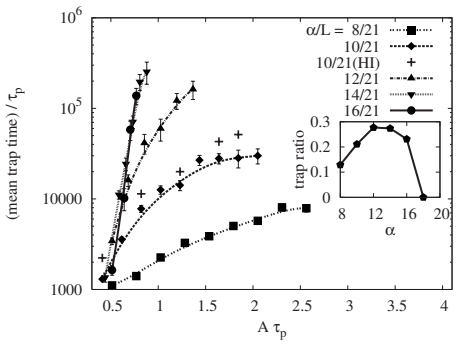


FIG. 3. Relationship between mean trap time of a polymer molecule and the normalized magnitude of flow field $A$. Here, $\tau_p = 4.1[\tau]$ is the relaxation time of the polymer [8], and $\alpha/L$ represents the ratio of the wavelength of the Taylor vortex flow (i.e., 2 $\times$vortex size) to the contour length of the polymer molecule. Data denoted by (+) symbols were obtained by BD simulations with hydrodynamic interactions, and others by free-draining BD simulations. Error bars indicate the standard errors. In the inserted figure, the trap ratio, which is the fraction of time a molecule is trapped, is shown for $A\tau_p = 0.7$.

The stability of the trapped state is dependent on the parameters of flow field, $A$ and $\alpha$ (see Fig. 3). We find that the trapped state is more stable for larger $A$ and that there is an optimal $\alpha$ that maximizes stability, which is around $\alpha = 12.0[l]$ for a molecule of contour length $21.0[l]$ with 10 beads. If $A$ is large and $\alpha$ is tuned for trapping, this can lead to "ergodicity breaking" where the trapped state and the tumbling state become separated from one another for very long times in the conformational phase space of the system [2]. The simplest example of ergodicity breaking was demonstrated by Schroeder *et al.* for a very long DNA molecule in extensional flow [1].

The stability of the trapped state can be explained by a simple local force balance along the molecule between the drag forces from the flow on the beads and the spring forces. As shown in Fig. 4, although the drag forces stretch the molecule and tend to pull it upwards, the spring forces acting along the curved contour of the molecule tend to pull the molecule back downwards and limit its stretch. The total spring force pulling the molecule toward the center of the curvature is the same force that induces radial migration of a polymer molecule in a curvilinear shearing flow such as a concentric cylinder or a cone-and-plate flow [9,10]. Here, however, this force is exactly balanced by the total drag force by the flow field, leading to both conformational and positional trapping.

Neglecting Brownian motion, the force balance along a polymer molecule in the trapped state can be expressed by the following equation:

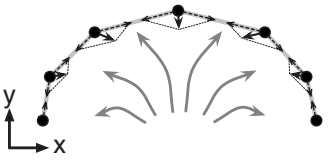


FIG. 4. Local force balance along a curved polymer molecule under fluidic stretching: the spring forces (black arrows) balance the drag forces exerted on beads by a solvent flow (gray arrows).

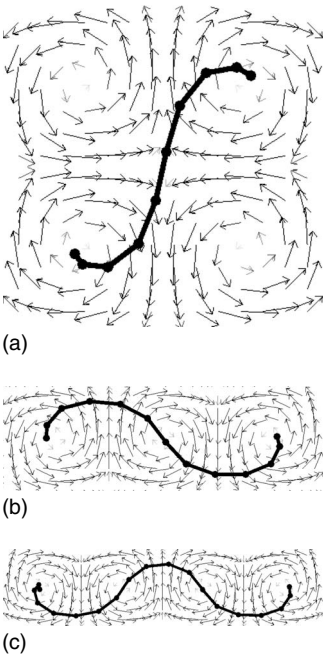


FIG. 5. Examples of stable conformations of polymer molecules in Taylor vortex flow for $A\alpha = 8.0[l/\tau]$ and $\alpha = 12[l]$. The number of beads is 10 in the top figure, 13 in the middle, and 19 in the bottom.

$$\boldsymbol{v}[\boldsymbol{r}(s)]\xi(s) + \frac{d}{ds}\left\{\frac{f^{sp}[\lambda(s)]}{\lambda(s)}\frac{d\boldsymbol{r}}{ds}\right\} = 0, \tag{9}$$

with boundary conditions

$$\left.\frac{d\boldsymbol{r}}{ds}\right|_{s=0} = \left.\frac{d\boldsymbol{r}}{ds}\right|_{s=L_p} = 0. \tag{10}$$

Here, $\boldsymbol{r}(s)$ is the position vector at $s$, which is a position coordinate along the polymer contour, $\boldsymbol{v}[\boldsymbol{r}(s)]$ is the velocity of solvent at position $\boldsymbol{r}(s)$, $\xi(s)$ is the drag coefficient per unit length of the polymer at $s$, $\lambda(s)$ is the local stretch of the polymer at $s$ and $L_p$ is the length of the polymer. The first term of the left side in Eq. (9) represents the drag force per unit length at position $\boldsymbol{r}(s)$ and the second term represents the derivative of the tension vector at the position, which produces a net migration force normal to the polymer contour. Solving Eq. (9) for a molecule modeled by our bead-spring model, we obtain the stable conformations in a Taylor vortex flow shown in Fig. 5. All of these conformations were confirmed to be stable enough to hold the molecule in fixed conformation and position even when Brownian motion is added. Note, however, that not all of these conformations were observed in the BD simulations because some of them have only a small chance of being accessed from an arbitrary starting state. When the size of the vortexes is much smaller than that of molecule (i.e. $\alpha \ll L$), the molecule can be trapped over multiple vortexes via stagnation points at the centers of the vortexes.

### B. Effect of hydrodynamic interactions

BD simulations with hydrodynamics interactions were also carried out to examine the effect on the trapping behav-

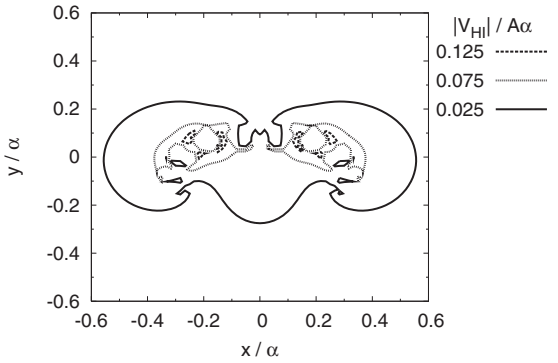


FIG. 6. The magnitude of flow perturbation velocity field $[\boldsymbol{V}_{\mathrm{HI}}(x,y)]$ induced by hydrodynamic interactions in the $x$-$y$ plane at $z=0$, where a polymer molecule is trapped. The directions of the $x$ and $y$ axes are the same as in Fig. 4 with respect to the conformation of the trapped polymer, and the origin $(x,y)=(0,0)$ is set to be the center of mass of the trapped polymer. Note that, in this plane, the flow perturbation velocity does not have a $z$ component and has only in-plane components.

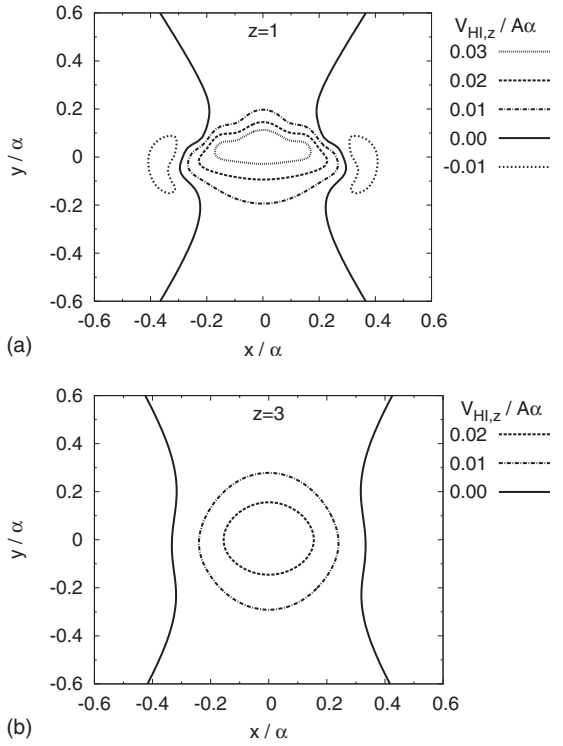


FIG. 7. The $z$ component of the flow perturbation velocity field $[V_{\mathrm{HI},z}(x,y)]$ in the $z=1$ plane (top) and $z=3$ (bottom) induced by hydrodynamic interactions from a polymer trapped in the $z=0$ plane. The directions of the $x$, $y$ axes and the origin are chosen as in Fig. 6. A positive $V_{\mathrm{HI},z}$ indicates a velocity away from the $z=0$ plane, where the trapped polymer resides.

ior in a Taylor vortex flow. The HIs between beads of a polymer molecule were computed using the Rotne-Prager-Yamakawa (RPY) tensor [11,12], and the details of this simulation are described in the Appendix. The simulation results show that HI does not significantly affect the trapping behavior but only produces a small variation from free-draining simulations in the mean trap times (Fig. 3). This is because the flow perturbation induced by HIs are not large enough, even in the trapped state, to significantly change the conformation of a polymer in the Taylor vortex flow. Figure 6 shows the flow perturbation by HIs in the $z=0$ plane, where a polymer is trapped, and the velocity induced by HIs is only 15% of the magnitude of the Taylor vortex flow $(A\alpha)$ at most, even very close to the polymer.

An interesting point to note here is that, when a polymer is trapped in the $x$-$y$ plane at $z=0$, the flow perturbation velocity field in an $x$-$y$ plane for $z\neq 0$ has a nonzero $z$ component of velocity. In other words, a two-dimensionally trapped polymer pushes solvent hydrodynamically along the $z$ axis. As shown in Fig. 7, the $z$ component of the flow perturbation is directed away from the trapping plane $(z=0)$ over most of the area, and decays with distance from the trapped polymer. Note that the flow perturbations were computed for a trapped polymer at the steady state without Brownian motion using the parameters $A\alpha=10.0[l/\tau]$, $\alpha=2.0[l]$, and $L=21.0[l]$ (10 beads).

These results imply that two trapped polymers close together in a Taylor vortex flow interact repulsively due to the induced HIs. We computed the velocity of center-of-mass migration by HIs in the $z$ direction for four different configurations of two simultaneously trapped polymers (Fig. 8). For all four configurations, two trapped polymers repel each other, and the repulsive velocity decays $\sim r_{12}^{-1.8}$ asymptotically, where $r_{12}$ is the distance between centers of mass of two trapped polymers. Therefore, if multiple polymers were simultaneously trapped in a microflow, they would tend to disperse in space and not concentrate.

### C. Trapping in an electro-osmotic flow

Conformational trapping of a polymer molecule is a general phenomenon that might occur for a deformable polymer molecule in a flow field that satisfies the conditions that there are at least two stagnation points and a net flow orthogonal to the line connecting them.

One well-defined geometry that creates such a flow is a electro-osmotic flow generated by an electric field $\boldsymbol{E}$ in a fluid bounded by surfaces bearing a charge varying sinusoidally in space, which was proposed by Ajdari [13]. Consider two flat insulating surfaces, defined as the $x=\pm h$ planes in a $(x,y,z)$ system of Cartesian coordinates, confining an electrolyte solution of Debye length $\kappa^{-1}$, dielectric constant $\epsilon$, and viscosity $\eta$. If the surfaces have a symmetric charge distribution: $\sigma^{+}(y)=\sigma^{-}(y)=\sigma_0\cos(qy)$, the stream function of the flow field $\phi(x,y)$, such that $\partial_x\phi=v_y$ and $\partial_y\phi=-v_x$, is expressed as

$$\phi(x,y)=\mu_0 E_y\cos(qy)\times\frac{h\cosh(qh)\sinh(qx)-x\sinh(qh)\cosh(qx)}{hq-\sinh(qh)\cosh(qh)} \tag{11}$$

in the limit of a thin Debye layer $\kappa\gg q,h^{-1}$, where $\mu_0=-\sigma_0/\eta\kappa$ and $E_y$ is the $y$ component of the electric field.

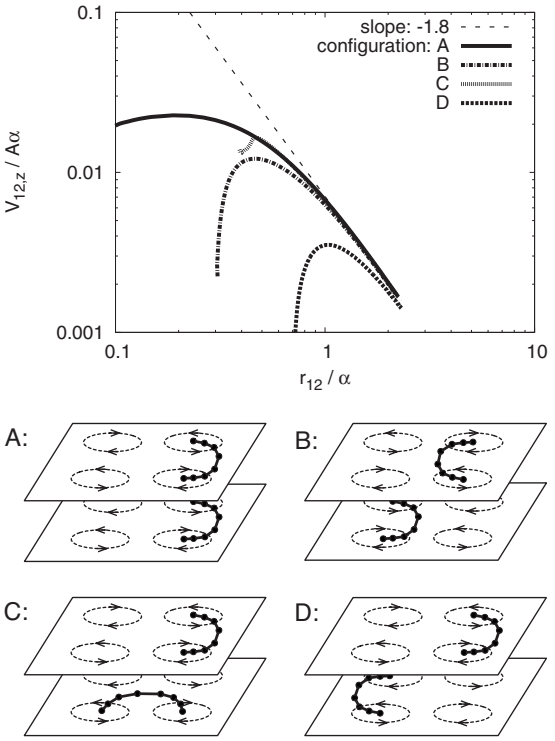


FIG. 8. Four configurations of two closely trapped polymers (bottom), and the $z$ component of the relative velocities of the two centers-of-mass $V_{12,z}$ induced by hydrodynamic interactions for each configurations (top). $r_{12}$ is the distance between the centers of mass. Note that a positive $V_{12,z}$ corresponds to chains moving away from each other.

From simulations using this geometry, we find that a neutral polymer molecule can be trapped in a similar way as in a Taylor vortex flow (see Fig. 9). Although Panwar *et al.* previously studied the polymer stretching behavior in the same geometry, their ratio of the size of the polymer molecule to channel width $2h$ was too small ($R_g/2h \simeq 10^{-3}$) for the flow to trap a polymer conformationally [14]. In our simulation, $R_g/2h \simeq 0.03$ was used.

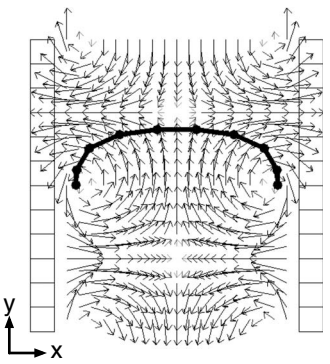


FIG. 9. Steady-state conformation of a trapped polymer in an electro-osmotic flow in a channel whose surfaces bear a sinusoidally varying charge: $\sigma^{\pm}(y)=\sigma_0 \cos(qy+\pi/4)$, where $\sigma_0$ was chosen to satisfy $\mu_0 E_y=7.0[l/\tau]$, and $q=2\pi/(2h)[l^{-1}]$, $h=6.0[l]$. The contour length of the polymer is $L=21[l]$ (10 beads). Despite the presence of arrows going into the wall, a thin boundary layer at the wall preserves the no-penetration boundary condition.

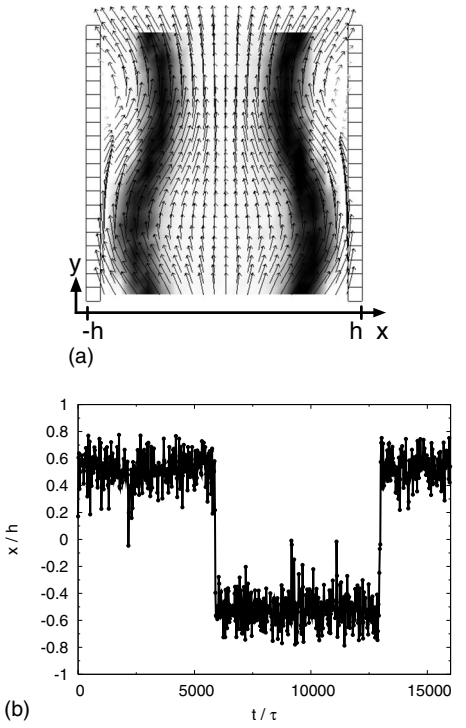


FIG. 10. The center-of-mass distribution marked as dark shading (top) and history of the center-of-mass position in $x$ direction (bottom) of a polymer molecule in an electro-osmotic flow in a channel whose surfaces bear a charge varying sinusoidally plus a net charge: $\sigma^{\pm}(y)=\sigma_0 \cos(qy+\pi/4)+\sigma_{\text{net}}$, where $\sigma_0$ and $\sigma_{\text{net}}$ were chosen to satisfy $\mu_0 E_y=4.0[l/\tau]$ and $\mu_{\text{net}} E_y=2.0[l/\tau]$, and $q=2\pi/(2h)[l^{-1}]$, $h=10[l]$. The contour length of the polymer is $L=63[l]$ (30 beads).

Moreover, when the surfaces of this channel have a net charge: $\sigma^{+}(y)=\sigma^{-}(y)=\sigma_0 \cos(qy)+\sigma_{\text{net}}$, the simulations show an inhomogeneous distribution of a neutral polymer molecule in the resulting electro-osmotic flow as shown in Fig. 10. The polymer molecule is trapped near either of the two streamlines that have a relatively large flow velocity and rarely seeps into the region between them. When trapped along a streamline, the molecule is stretched along the streamline most of the time and we observed a conformation similar to the trapped state shown previously in the Taylor vortex flow, but here, because of a net flow, the conformation changes periodically and the motion resembles that of a swimming sea snake.

Note that the surfaces have a sinusoidal charge plus a net charge, which is equivalent to surfaces having only a sinusoidal charge but a polymer molecule having a charge, whose electrophoretic mobility is $\mu_p=\sigma_{\text{net}}/\eta\kappa$.

## IV. SUMMARY AND DISCUSSION

Our simulations suggest the possibility of single-molecule trapping and stretching using only a fluid flow such as a microflow with multiple vortexes. Using such a flow, a polymer molecule can be trapped spatially and conformationally without external force or physical constraint. The stability of the trapped state of a molecule can be optimized by tuning

the parameters of the flow field, namely the magnitude and the size of the vortexes.

The trapped state is stabilized by two key dynamics of the polymer: the coil-stretch transition and the center-of-mass migration in a curved streamline. The conformational trap is triggered by the coil-stretch transition that separates two conformational states of a polymer molecule in the conformation phase space. The positional trap is realized by a balance between the migration induced by the drag force on the molecule and the center-of-mass migration in a curved streamline, which is also observed in a curvilinear shear flow such as a cone-and-plane flow.

Note that microflows with multiple vortexes have been used to mix solutions in a microchannel [15]. Our study suggests that this flow could also demix or concentrate polymer molecules when the length scale of the molecule size is comparable to, or larger than the vortex size. This effect could be utilized for separation of polymer molecules from small molecules, such as separation of DNA from proteins.

## ACKNOWLEDGMENT

We acknowledge support from the NSF under Grant No. NSEC EEC-0425626

## APPENDIX: BROWNIAN DYNAMICS WITH HYDRODYNAMIC INTERACTIONS

To describe Brownian dynamics simulations with hydrodynamics interactions between the beads of the polymer, we replace Eq. (5) by [16]:

$$\boldsymbol{r}_i(t+\delta t)-\boldsymbol{r}_i(t)=\left\{\boldsymbol{v}_i(\boldsymbol{r}_i)+\sum_{j=1}^{N}\frac{\partial \mathcal{D}_{ij}}{\partial \boldsymbol{r}_j}+\sum_{j=1}^{N}\frac{\mathcal{D}_{ij}\cdot\boldsymbol{f}_j}{k_BT}\right\}\delta t + \sqrt{6\delta t}\sum_{j=1}^{i}\mathcal{B}_{ij}\cdot\boldsymbol{n}_j, \tag{12}$$

where $\mathcal{D}(=\mathcal{B}\cdot\mathcal{B}^T)$ is the RPY tensor described as follows [8,11,12]:

$$\mathcal{D}_{ii}=\frac{k_BT}{\xi}\mathcal{I}, \tag{13}$$

$$\mathcal{D}_{ij}=\frac{k_BT}{\xi}\frac{3a}{4r_{ij}}\left[C_1\mathcal{I}+C_2\frac{\boldsymbol{r}_{ij}\boldsymbol{r}_{ij}}{r_{ij}^2}\right] \quad \text{if } i\neq j \text{ and } r_{ij}\geqslant 2a, \tag{14}$$

$$\mathcal{D}_{ij}=\frac{k_BT}{\xi}\left[\left(1-\frac{9r_{ij}}{32a}\right)\mathcal{I}+\frac{3}{32}\frac{\boldsymbol{r}_{ij}\boldsymbol{r}_{ij}}{ar_{ij}}\right] \quad \text{if } i\neq j \text{ and } r_{ij}<2a, \tag{15}$$

$$C_1=1+\frac{2a^2}{3r_{ij}^2}, \tag{16}$$

$$C_2=1-\frac{2a^2}{r_{ij}^2}. \tag{17}$$

Here, $\boldsymbol{r}_{ij}=\boldsymbol{r}_i-\boldsymbol{r}_j$, $\mathcal{I}$ is the $3\times 3$ identity matrix, $a$ is the radius of a bead and $\xi$ is the drag coefficient of a bead. The parameters $a=0.077[l]$ and $\xi=15.4[k_BT\tau/l^2]$ were used to make the relaxation time and the diffusivity of the polymer equivalent to those of the free-draining BD simulation [8]. Note that the gradient of $\mathcal{D}_{ij}$ [the second term in the right-hand side of Eq. (12)] vanishes for the RPY tensor.

[1] C. M. Schroeder, H. P. Babcock, E. S. G. Shaqfeh, and S. Chu, Science **301**, 1515 (2003).
[2] V. A. Beck and E. S. G. Shaqfeh, J. Chem. Phys. **124**, 094902 (2006).
[3] J. Kreft, Y. L. Chen, and H. C. Chang, Phys. Rev. E **77**, 030801(R) (2008).
[4] G. I. Taylor, Philos. Mag. **46**, 671 (1923).
[5] D. L. Ermak and J. A. McCammon, J. Chem. Phys. **69**, 1352 (1978).
[6] R. G. Larson, T. T. Perkins, D. E. Smith, and S. Chu, Phys. Rev. E **55**, 1794 (1997).
[7] J. F. Marko and E. D. Siggia, Macromolecules **28**, 8759 (1995).
[8] R. Jendrejack, J. J. de Pablo, and M. D. Graham, J. Chem. Phys. **116**, 7752 (2002).
[9] K. A. Dill and B. H. Zimm, Nucleic Acids Res. **7**, 735 (1979).
[10] R. G. Larson, Rheol. Acta **31**, 497 (1992).
[11] J. Rotne and S. Prager, J. Chem. Phys. **50**, 4831 (1969).
[12] H. Yamakawa, J. Chem. Phys. **53**, 436 (1970).
[13] A. Ajdari, Phys. Rev. Lett. **75**, 755 (1995).
[14] A. S. Panwar and S. Kumar, J. Chem. Phys. **118**, 925 (2003).
[15] A. D. Strook, S. K. W. Dertinger, A. Ajdari, I. Mezic, H. A. Stone, and G. M. Whitesides, Science **295**, 647 (2002).
[16] C. Hsieh, L. Li, and R. G. Larson, J. Non-Newtonian Fluid Mech. **113**, 147 (2003).